



Experiment title:

Structure and Dynamics of Confined Liquids Studied by X-Ray Scattering

Experiment number:

MI-1217

Beamline:

ID31

Date of experiment:

from: 23/02/2016 to: 01/03/2016

Date of report:

20.08.2016

Shifts:

18

Local contact(s):

Veijo Honkimäki

Received at ESRF:

Names and affiliations of applicants (* indicates experimentalists):

Mezger, Markus^{1*}; Weiss, Henning^{1*}; Li, Hailong^{1*}; Mars, Julian^{1*}; Valtiner, Markus^{2*}; Cheng, Hsiu-Wei^{2*}; Buvaneswaran, Sadhanaa^{2*}; Merola, Claudia^{2*}

1 Max-Planck-Institut für Polymerforschung, 55128 Mainz, Germany

2 Max-Planck-Institut für Eisenforschung, 40237 Düsseldorf, Germany

Report:

Confined liquids play an important role in many technical applications and processes. Studies on the performance of batteries and capacitors showed that electrochemical [1, 2] and catalytic processes [3] are sensitive to the molecular scale liquid structure adjacent to interfaces. In these applications, liquids are often present in a nano-porous matrix, increasing the interfacial area. Thus, a detailed knowledge of the structure of confined liquids on molecular length scale is of great interest for fundamental and applied sciences.

The Surface Force Apparatus (SFA) is an established experimental setup to control the distance between two surfaces approaching each other on a range from micrometers down to nanometers. Therefore, this instrument can be used to create a controlled slit-pore confinement with dimensions on the molecular length scale [4]. X-ray scattering and reflectivity (XRR) are powerful techniques to probe structures on molecular scale in bulk and at interfaces. In our proof of principle experiment MI-1217 at ID31 in February/March 2016 we successfully combined these two complementary techniques to a novel type of a dynamic X-ray Surface-Force-Apparatus (XSFA, Fig. 1). Our first results confirm that the instrument is sensitive to study the anisotropic structure of a confined liquid crystal and its response to dynamic compression.

The XSFA uses white light interference between two semipermeable mirrors to measure the distance between two atomically flat surfaces. Fringes of equal chromatic order (FECO) are detected by a spectrometer (Fig. 1a). The confined area is monitored and aligned with respect to the X-ray beam by video microscopy (Fig. 1b). The liquid is confined between a planar corundum block (Al_2O_3 , upper surface) and cylindrical mica sheet (lower surface) that is aligned perfectly parallel to the corundum block (see FECO in Fig. 1a). This configuration provides a confinement over a much larger area compared to the conventional crossed cylinder geometry. With our instrument, we are able to align the confined region along the beam, probing a volume of $300 \mu\text{m}$ width, 5 mm length and adjustable height. At $2 \mu\text{m}$ slit-pore gap width, a total volume of $3 \cdot 10^{-3} \text{ mm}^3$ is probed by the X-ray beam. This is about ten times the volume probed by other XSFA setups in reflection geometry (e.g. Ref. 5). The lower mica surface can be moved vertically by a piezo stage with nanometer precision (Fig. 1c). For dynamic studies,

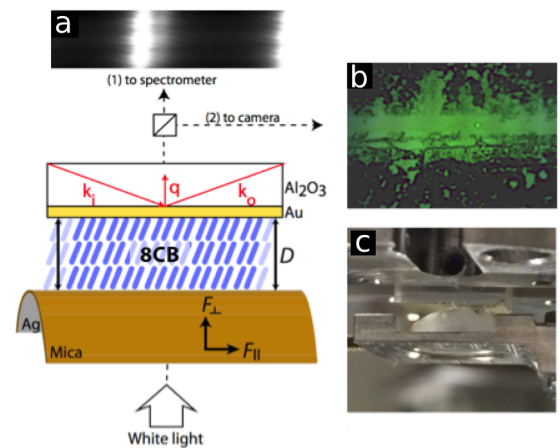


Figure 1: Sketch of our XSFA setup. (a) Interference fringes of equal chromatic order are used to determine the gap width. (b) Top-view of the confined 8CB by video microscopy indicating perfect parallel alignment of the apposing surfaces. (c) Photograph of the slit pore confinement generated by a planar corundum block (Al_2O_3 , top) and a mica sheet mounted on a cylindrical glass holder (bottom).

oscillatory stress can be applied to the sample by the piezo controller. For optical interference measurements, the lower and upper surfaces were coated with semi-transparent mirrors. Corundum blocks were covered with a 40 nm template stripped gold layer of atomic scale roughness. A silver film was evaporated on the backside of the mica sheet. Subsequently the mica was mounted on a round glass holder to produce a cylindrically shaped lower surface. The liquid sample was injected between the surfaces by a needle. During the measurement the liquid is held in place by adhesion forces. To probe the buried solid/liquid interface a 70 keV X-ray beam with $5 \times 20 \mu\text{m}$ size impinges the sample through the single-crystalline corundum block. Compared to amorphous substrate materials, this significantly reduced background scattering. The profile perpendicular to the confining interfaces is investigated by XRR. Scattering experiments with a momentum transfer parallel to the slit pore probe the in-plane structure of the liquid (Fig. 2). For sample positioning and orientation, the device was mounted on the High Energy Micro Diffractometer (HEMD) setup at ID31. The scattered and reflected X-rays were detected by a CdTe MAXIPIX detector with $55 \mu\text{m}$ pixel size.

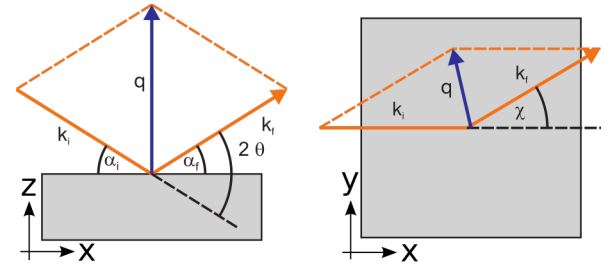


Figure 2: Scattering geometry for X-ray reflectivity with the momentum transfer q perpendicular to the solid/liquid interface (left) and in-plane scattering geometry with the momentum transfer parallel to the solid/liquid interface (right).

As a model system, we choose the liquid crystal 4'-octyl-4-cyano-biphenyl (8CB). At 22°C , 8CB exhibits a smectic A phase. The arrangement of the rod-like molecules in smectic layers gives rise to a pronounced scattering peak in the small angle scattering (SAXS) regime (Fig. 3a). To induce a defined orientation of the 8CB molecules at the lower and upper interface, both surfaces were hydrophobized by a self-assembled monolayer of hexadecane-thiol and perfluorosilane respectively. During the XRR and in-plane scattering experiments, the liquid crystal was confined to a gap width of $1.7 \mu\text{m}$.

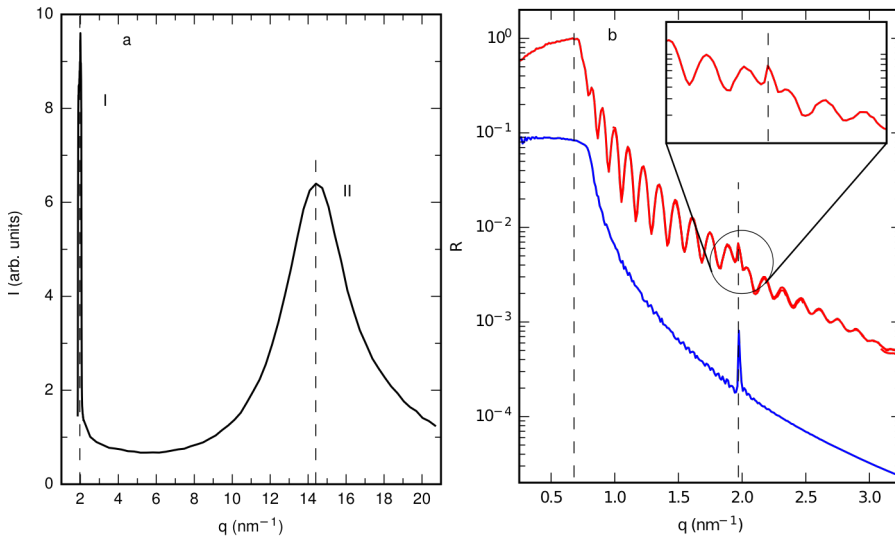


Figure 3: Scattering signal from confined 8CB. (a) In-plane pattern recorded in the scattering geometry depicted in the right panel of Fig. 2. (b) Measured (red) specular X-ray reflectivity R . Model calculated reflectivity curve (blue) from a periodic arrangement of 500 smectic 8CB layers arranged parallel to the solid/liquid interface. For clarity, curves are shifted vertically by 1 order of magnitude.

Figure 3 summarizes the experimental data obtained from confined 8CB in the in-plane scattering (a) and XRR geometry (b) depicted in Fig. 2. In the in-plane scattering geometry the structure in the x - y -plane i.e. parallel to the solid/liquid interface is probed. The scattering pattern exhibits a sharp peak (I) at $q = 2.0 \text{ nm}^{-1}$. The corresponding real space distance of 3.3 nm is in good agreement with the periodicity of the smectic mesophase of 8CB found by SFA experiments [6]. The observed peak shape is consistent with quasi long range liquid crystalline smectic order. A second, broad peak (II) appears around 14 nm^{-1} . This length scale of approx. 0.45 nm corresponds to the short distance between the rod-like 8CB molecules within the smectic layers. The large FWHM of 4 nm^{-1} originates from the short range order perpendicular to the long axis of the molecules.

The density profile perpendicular the solid/liquid interface is probed by XRR (Fig. 2 left and red curve in Fig. 3b). The critical angle of total reflection at 0.7 nm^{-1} is determined by the large scattering contrast between the gold mirror and the upper corundum block. At higher q , the x-ray beam is transmitted into the gold layer and the slit-pore filled with 8CB. Kiessig fringes of periodicity $\Delta q = 0.15 \text{ nm}^{-1}$ originate from interference at the 40 nm thick gold mirror. At approx. 2 nm^{-1} a sharp Bragg-like peak is observed in the XRR curve. Like the first peak observed in the in-plane scattering geometry, this reflection is attributed to the smectic order of the confined 8CB. The blue curve shows the calculated XRR based on a simplified model consisting of 500 smectic 8CB layers with 3.2 nm periodicity on top of a semi infinite gold substrate. Refractive indices were calculated using the CXRO database, taking into account the chemical structure of 8CB.

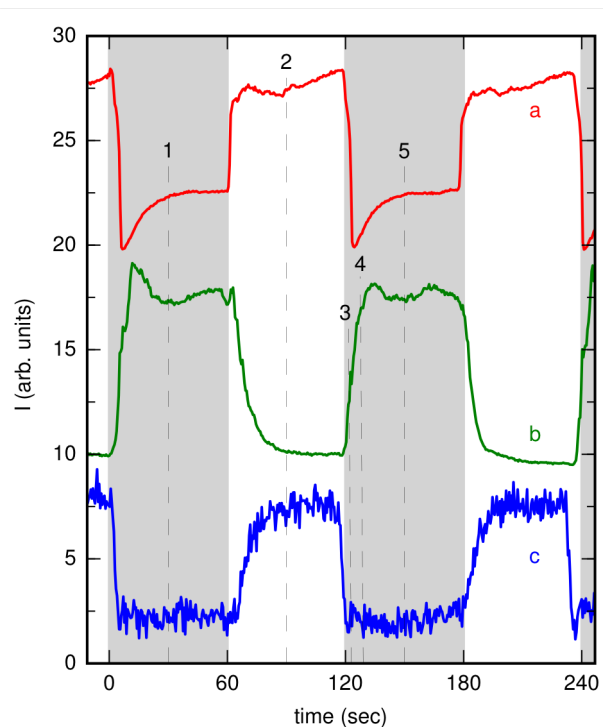


Figure 4: Response of the scattering signal from the confined liquid crystal 8CB structure to externally applied compressive strain. Grey shaded areas indicate decompression, white areas compression. (a, red) Modulation of the specular XRR and in-plane signals at the first sharp (b, green) and second diffuse (c, blue) scattering peaks. Curves are scaled and vertically shifted.

modulation. This is explained by the perpendicular arrangement of the long and short axis in the 8CB molecules. While the XRR signal increases promptly, a similar time scale on the order of 10 s was observed for the relaxation of both in-plane scattering signals under compressive stress. When the gap opens at $t = 0$ s, additional 8CB molecules flow into the confinement zone. This leads to a more isotropic distribution of the smectic layer orientation and therefore a rapid decrease of the XRR signal. The following slow increase over a 30 s time period indicates that the orientation of the smectic layers is gradually restored. However, over the studied time scales, it never reaches the values found after compression of the confined 8CB molecules. As observed for the compression, the drop in XRR intensity upon decompression is accompanied by an increasing and decreasing first and second in-plane scattering peak, respectively. This periodic process is reproducibly repeated over several compression/decompression cycles.

The structural relaxation upon compression and decompression can be followed in more detail by analyzing the time sequence of the 2D scattering patterns. Figure 5 shows a selection of 2D data recorded around the specular condition (upper row) and in the in-plane scattering geometry (lower row) at times indicated by the vertically dashed lines in Fig. 4. Upon decompression (1 and 5) the arc around the specular condition stretches out over the diffraction ring. Accordingly, we observe an increase in the in-plane direction compared to time point 2.

These results obtained for the liquid crystal 8CB in its smectic A mesophase proof that with our new XSFA we can create a control confinement on a micrometer length scale and probe the molecular order and orientation of confined liquids by X-ray scattering techniques. Our setup is not only limited to static measurement. The particular strength of our instrument are dynamic experiments on confined liquids that are brought out of equilibrium by compression and decompression of the slit-pore. Future improvements include the extension of the XSFA by Piezo-stages to apply horizontal shear stress, and a more precise force control in the confinement.

[1] A. Lee et al., *Nanotechnology* 25, 315401 (2014).
 [2] C. Largeot et al., *J. Am. Chem. Soc.* 130, 2730 (2008).
 [3] A. Riisager et al., *Ind. Eng. Chem. Res.* 44, 98532005 (2005).

The scattered intensity found in the specular condition i.e. with the momentum transfer perpendicular to the solid/liquid interface (z-direction), is orders of magnitudes stronger than the intensities found for other directions (Fig. 5). This angular intensity distribution over the scattering rings of constant total momentum transfer is caused by an anisotropic structure caused by the confinement. The observed patterns indicate that the smectic layers of the confined 8CB are preferably oriented parallel to the hydrophobic functionalized lower and upper solid/liquid interfaces. This structure is now brought out of equilibrium by periodic compression and decompression of the slit-pore confinement. Changes in the gap width are directly monitored by the FECO interference pattern. By applying a step signal of ∓ 2 V with 60 s periodicity to the piezos we obtain an amplitude of about 10 nm. While this value corresponds to only 3 out of 560 smectic 8CB layers pronounced modulations were observed in the XRR and in-plane scattering signal. Figure 4 summarizes the time evolution over two compression/decompression cycles indicated by the white and grey shaded areas. The red and green curves show the time dependence of the scattering signal at the sharp first peak for a momentum transfer pointing in the z (specular XRR) and x-y (in-plane) direction, respectively. Upon compression at $t = 60$ s, intensity is shuffled from the x-y to the z direction. This indicates that compressive stress is increasing the alignment of the liquid crystalline smectic layers relative to the confining solid interfaces. This increases the anisotropy in the angular intensity distribution. Accordingly, the intensity of the second broad scattering peak at $q_{xy} = 14 \text{ nm}^{-1}$ detected in the in-plane geometry (blue curve) shows the opposite signal

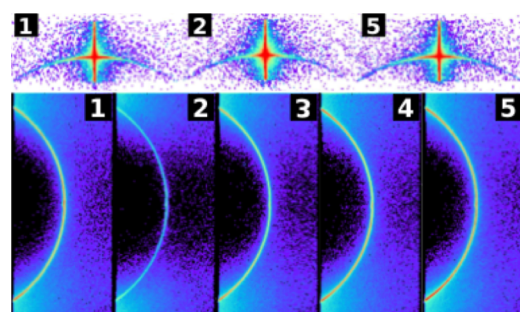


Figure 5: 2D scattering patterns during periodic compression and decompression cycles. Near specular intensity distribution around the first order Bragg reflection from the smectic order at $q_z = 2 \text{ nm}^{-1}$ (top) and in the in-plane scattering geometry (bottom). Numbers refer to times indicated

[4] J. Israelachvili, et al., *Rep. Prog. Phys.* 73, 036601 (2010).
 [5] E. Perrett, Dissertation ETH Zürich, Nr. 18982 (2010).
 [6] M. Ruths et al., *Langmuir* 12, 6637 (1996).